CFD Letters

Journal homepage:
https://semarakilmu.com.my/journals/index.php/CFD_Letters/index
ISSN: 2180-1363

Consequences of Thermal Diffusion and Chemical Reaction on Mixed Convection MHD Casson Fluid through Porous Media with Inclined Plates

Sunita Rani Yedhiri[1], Srinivasa Rao Puchakayala[2], Kalyan Kumar Palaparthi[3], Haribabu Kommaddi[3,*]

[1] Department of Mathematics, CMR Engineering College (Autonomous), Hyderabad, 501401, India
[2] Department of Mathematics, Malla Reddy Engineering College (Autonomous), Dhulapally. Hyderabad 500100, India
[3] Department of Engineering Mathematics, Koneru Lakshmaiah Education Foundation, Hyderabad, 500075, Telangana, India

ARTICLE INFO

Article history:
Received 13 October 2023
Received in revised form 15 November 2023
Accepted 12 December 2023
Available online 30 April 2024

Keywords:
Thermal diffusion; inclined plates; chemical reaction; porous media; heat and mass transfer

ABSTRACT

In this present article, we analyzed the effects of Thermal diffusion and chemical reaction on nonlinear mixed convection MHD flow of viscous, incompressible and electrically conducting fluid past an inclined porous channel under the influence of thermal radiation and chemical reaction. The transformed conservation equations are solved analytically subject to physically appropriate boundary conditions by using two term perturbation technique. The numerical values of fluid velocity, fluid temperature and species concentration are displayed graphically whereas those of skin friction coefficient, rate of heat transfer and rate of mass transfer at the plate are presented in tabular form for various values of pertinent flow parameters. It is observed that the velocity is decreased with increasing magnetic field parameter. The resultant velocity and concentration has enhances with increasing thermal diffusion parameters. The study is relevant to chemical materials processing applications.

1. Introduction

The convective heat and mass transfer flows in an inclined porous plate find a number of applications in many branches of science and technology like chemical industry, cooling of nuclear reactors. MHD power generators, geothermal energy extractions processes, petroleum engineering etc. The hydro magnetic convection with heat and mass transfer in porous medium has been studied. It is due to its importance in the design of MHD generators, accelerators in geophysics, the design of underground water energy storage system, soil-sciences, astrophysics, nuclear power reactors and so on. In nature, there be flows which are affected not simply by the temperature differences however furthermore by the concentration differences. These mass transfer differences do effects the *rate* of heat transfer. In Industries, many transport processes exist in which heat and mass transfer takes place simultaneously as a result of combined buoyancy effect

* *Corresponding author.*
E-mail address: mathematicshari@gmail.com (Haribabu Kommaddi)

https://doi.org/10.37934/cfdl.16.9.6480

in the presence of thermal radiation. If the temperature of surrounding fluid is rather high, the radiation effects play an important role and this situation does exist in space technology.

Magneto hydrodynamics is currently undergoing a period of great enlargement and differentiation of subject matter. The interest in these new problems generates from their importance in liquid metals, electrolytes and ionized gases. Heat source and chemical effects on MHD convection flow embedded in a porous medium with Soret, viscous and Joules dissipation has been investigated quite extensively Raghunath *et al.,* [1] have studied Hall current and thermal radiation effects of 3D rotating hybrid nanofluid reactive flow via stretched plate with internal heat absorption. Raghunath *et al.,* [2] have studied unsteady magneto-hydro-dynamics flow of Jeffrey fluid through porous media with thermal radiation, Hall current and Soret effects. Raju *et al.,* [3] have studied Chemical Radiation and Soret Effects on Unsteady MHD Convective Flow of Jeffrey Nanofluid Past an Inclined Semi-Infinite Vertical Permeable Moving Plate. Ramachandra *et al.,* [4] have reviewed Effects of Hall Current, Activation Energy and Diffusion Thermo of MHD Darcy-Forchheimer Casson Nanofluid Flow in the Presence of Brownian motion and Thermophoresis. Raghunath *et al.,* [5] have possessed processing to pass unsteady MHD flow of a second-grade fluid through a porous medium in the presence of radiation absorption exhibits Diffusion thermo, hall and ion slip effects. Very Recently Li *et al.,* [6] have expressed Effects of activation energy and chemical reaction on unsteady MHD dissipative Darcy–Forchheimer squeezed flow of Casson fluid over horizontal channel. Suresh Kumar *et al.,* [7] have observed Numerical analysis of magnetohydrodynamics Casson nanofluid flow with activation energy, Hall current and thermal radiation.

Combined heat and mass transfer problems with chemical reaction are of importance in many processes and have, therefore, received a considerable amount of attention in recent years. In processes such as drying, evaporation at the surface of a water body, energy transfer in a wet cooling tower and the flow in a desert cooler, in chemical reaction engineering heat and mass transfer occur simultaneously. Raghunath *et al.,* [8] have analyzed Diffusion Thermo and Chemical Reaction Effects on Magnetohydrodynamic Jeffrey Nanofluid over an Inclined Vertical Plate in the Presence of Radiation Absorption and Constant Heat Source. Maatoug *et al.,* [9] have possessed Variable chemical species and thermo-diffusion Darcy–Forchheimer squeezed flow of Jeffrey nanofluid in horizontal channel with viscous dissipation effects. Omar *et al.,* [10] have reviewed Hall Current and Soret Effects on Unsteady MHD Rotating Flow of Second-Grade Fluid through Porous Media under the Influences of Thermal Radiation and Chemical Reactions. Deepthi *et al.,* [11] have studied Recent Development of Heat and Mass Transport in the Presence of Hall, Ion Slip and Thermo Diffusion in Radiative Second Grade Material: Application of Micromachines. Aruna *et al.,* [12] have examined an unsteady MHD flow of a second-grade fluid passing through a porous medium in the presence of radiation absorption exhibits Hall and ion slip effects. Raghunath *et al.,* [13] reviewed Hall, Soret, and rotational effects on unsteady MHD rotating flow of a second-grade fluid through a porous medium in the presence of chemical reaction and aligned magnetic field. Raghunath *et al.,* [14] have examined Hall and ion slip radiative flow of chemically reactive second grade through porous saturated space via perturbation approach.

The Soret effect arises when the mass flux contains a term that depends on the temperature gradient. The major focus of our study is the effect on mixed convection flow of the addition of a second fluid. Ramachandra *et al.,* [15] have studied Characteristics of MHD Casson fluid flow past an inclined vertical porous plate. Raghunath *et al.,* [16] have analyzed Effects of Radiation Absorption and Aligned Magnetic Field on MHD Cassion Fluid Past an Inclined Vertical Porous Plate in Porous Media. Unsteady MHD radiative and chemically reactive natural convection flow near a moving vertical porous plate through porous medium was studied by Reddy *et al.,* [17]. MHD convective and dissipative fluid flow over porous medium in a flat channel with insulated and impermeable bottom wall in the presence of Joule heating was considered by Raju *et al.,* [18]. Ravikumar *et al.,* [19] discussed the combined effects of heat absorption and magneto convective flow of a non-Newtonian fluid namely, Rivlin-Ericksen flow past a semi-infinite vertical porous plate. Exact solutions for MHD free convictive boundary layer flow past a porous vertical surface in the presence of chemical reaction, thermal radiation and suction were carried out by Raju *et al.,* [20].

The aim of the present work was to investigate the effects of thermal diffusion and chemical reaction on MHD mixed convective flow past an inclined plate embedded in a porous medium in the presence of heat source and aligned magnetic field. This is an extension to the work of Raghunath *et al.,* [15], this is not a simple extension of the previous work it differs in several aspects.

2. Physical Configuration and Mathematical Formulation

A steady MHD laminar mixed convective flow of a viscous, incompressible electrically conducting fluid along a semi-infinite inclined porous plate with an acute angle α to the considered. The physical coordinates (x,y) are chosen such that x is measured from the leading edge in the stream wise direction and y is measured normal to the surface of the plate. The velocity components in the directions of flow and normal to the flow are u and v respectively. A magnetic field of uniform strength B_0 is applied normal to the direction of flow. The external flow with a uniform velocity U_∞ takes place in the direction parallel to the inclined plate. It is assumed that T and C are the temperature and concentration of the fluid which are the same, everywhere in the fluid. The surface is maintained at a constant temperature T_w, which is higher than the constant temperature T_∞ of the surrounding fluid and the concentration C_w, is greater than the constant concentration C_∞. The schematic view of flow configuration and coordinates system is shown in Figure 1. The governing equations of continuity, momentum, energy and mass for a flow of an electrically conducting fluid are given by the following.

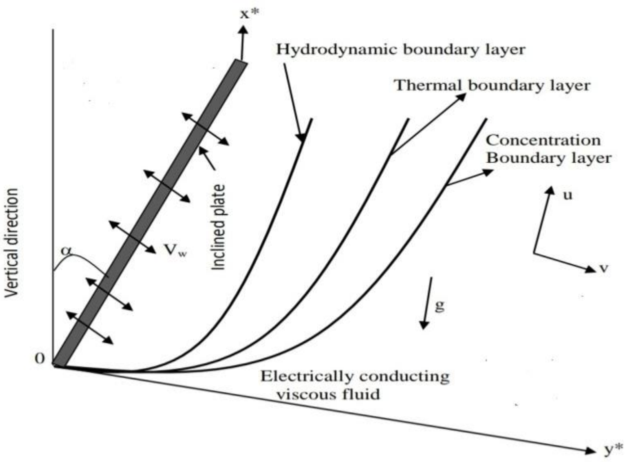

Fig. 1. Physical configuration of the problem

$$\frac{\partial v*}{\partial y*} = 0 \rightarrow v^* = -v_0 (v_0 > 0) \tag{1}$$

$$v*\frac{\partial u*}{\partial y*} = \vartheta\left(1+\frac{1}{\lambda}\right)\frac{\partial^2 u*}{\partial y*^2} + g\beta(T*-T_\infty)Cos\alpha + gB^*(C*-C_\infty)Cos\alpha - \frac{\sigma B_0^2}{\rho}Sin^2\gamma\, u* - \frac{\vartheta u*}{k^*} \tag{2}$$

$$v^*\frac{\partial T^*}{\partial y^*}=\frac{k}{\rho C_p}\frac{\partial^2 T^*}{\partial y^{*2}}+\frac{\vartheta}{C_p}\left(\frac{\partial u^*}{\partial y^*}\right)^2+\frac{\sigma B_0^2}{\rho}u^{*2}-\frac{1}{\rho C_p}\frac{\partial q_r^*}{\partial y^*}+\frac{Q_0}{\rho C_p}(T^*-T_\infty^*) \tag{3}$$

$$v^*\frac{\partial C^*}{\partial y^*}=D\frac{\partial^2 C^*}{\partial y^{*2}}+D_1\frac{\partial^2 T^*}{\partial y^{*2}}-K_1(C^*-C_\infty) \tag{4}$$

Where u* and v* are the components of velocity in x* and y* directions, respectively, taken along and perpendicular to the plate, g is the acceleration due to gravity, b is the coefficient of thermal expansion, b* is the coefficient of mass expansion, T* is the temperature of the fluid, T* is the temperature far away from the plate, Tw is the temperature near the plate. C* is the concentration of the fluid, C_w is the concentration near the plate, C_1 is the concentration far away from the plate, t is the kinematic viscosity of the fluid, r is the magnetic permeability of the fluid, k* is the permeability of porous medium, q is the fluid density, B_0 is the magnetic field coefficient, C_p is the specific heat of the fluid at constant pressure, v_0 is the constant suction velocity, D is the chemical molecular diffusivity, α is inclined parameter and k_1 is the chemical reaction rate constant.

The boundary conditions for the velocity, temperature and concentration fields are

$$u^*=0 \quad T^*=T_w, \quad C^*=C_w \quad \text{at } y^*=0$$

$$u^*\to 0, \quad T^*\to T_\infty \quad C^*\to C_\infty \quad \text{as} \quad y^*\to\infty \tag{5}$$

The radiative heat flux term by using Rosseland approximation q_r^*, takes the form

$$\frac{\partial q_r^*}{\partial y^*}=4\left(T^*-T_w^*\right)I$$

Where $I=\int_0^\infty K_{\lambda\omega}\left(\frac{\partial_{eb\lambda}}{\partial T}\right)_\omega d\lambda,\ K_{\lambda\omega}$ the absorption coefficient at the wall and ebλ is Planck's function.

On introducing the following non-dimensional quantities,

$$u=\frac{u^*}{v_0},\ y=\frac{v_0 y^*}{\vartheta},\ \Pr=\frac{\vartheta\rho C_p}{k},\ \theta=\frac{T^*-T_\infty}{T_w-T_\infty},\ \varphi=\frac{C^*-C_\infty}{C_w-C_\infty},\ Gr=\frac{\vartheta g\beta\ (T_w-T_\infty)}{v_0^3},$$
$$Gm=\frac{\vartheta g\beta_c^*(C_w-C_\infty)}{v_0^3},\ Ec=\frac{v_0^2}{C_p(T_w-T_\infty)},\ M^2=\frac{\sigma B_0^2\vartheta}{\rho v_0^2},\ k^*=\frac{\vartheta^2}{K_0 v_0^2},\ \vartheta=\frac{\mu}{\rho},\ S_c=\frac{\vartheta}{D} \tag{6}$$
$$S_0=\frac{D_1(T_w-T_\infty)}{\vartheta(C_w-C_\infty)},\ Kr=\frac{\vartheta K_1}{v_0^2},\ Q=\frac{Q_{0\vartheta}}{\rho C_p v_0^2},\ F=\frac{4I_1\upsilon}{\rho C_p v_0^2}.$$

where Gr is the Grashof number, Gm is the mass Grashof number, Pr is the Prandtl number, Sc is the Schmidt number, So is the Soret number, Ec is the Eckert number, M is the magnetic parameter, Ko

is the permeability of porous medium and Kr is the chemical reaction parameter, F is the thermal radiation parameter.
The basic field Eq. (2) – (4), can be expressed in non- dimensional form as

$$\frac{\partial u^2}{\partial y^2}\left(1+\frac{1}{\lambda}\right)+\frac{\partial u}{\partial y}-(M^2\,Sin^2\gamma-K_0)u=-G_r\,\theta\,Cos\alpha-G_m\,\varphi\,Cos\alpha \tag{7}$$

$$\frac{\partial^2\theta}{\partial y^2}+\Pr\frac{\partial\theta}{\partial t}+\Pr E_c\left(\frac{\partial u}{\partial y}\right)^2+\Pr Ec\,M^2u^2+\Pr(F+Q)\,\theta=0 \tag{8}$$

$$\frac{\partial^2\varphi}{\partial y^2}+Sc\frac{\partial\varphi}{\partial t}-Sc\,Kr\,\varphi+S_0\,S_c\,\frac{\partial^2\theta}{\partial y^2}=0 \tag{9}$$

The corresponding boundary conditions in dimensionless form are reduced to

$$\text{At } y^*=0,\quad u=0,\quad \theta=1,\quad \varphi=1$$

$$\text{As } y^*\to\infty,\ u\to 0,\quad \theta\to 1,\quad \varphi\to 1 \tag{10}$$

3. Solution of the Problem

Eq. (7) – Eq. (9) represent a set of partial deferential equations that cannot be solved in closed form. However, it can be reduced to a set of ordinary deferential equations in dimensionless form that can be solved analytically. This can be done by representing the velocity, temperature and concentration as;

$$\begin{aligned} u(y,t)&=u_0(y)+E_c u_1(y)+O(Ec^2)\\ \theta(y,t)&=\theta_0(y)+E_c\theta_1(y)+O(Ec^2)\\ \phi(y,t)&=\phi_0(y)+E_c\,\phi_1(y)+O(Ec^2)\end{aligned} \tag{11}$$

Using Eq. (11) in Eq. (7) – Eq. (9) and equating the coefficient of like powers of Ec, we have

3.1 Zero Order Terms

$$u_0''\left(1+\frac{1}{\lambda}\right)+u_0'-(\mathrm{M}^2\,Sin^2\gamma+\mathrm{K}_0)\mathrm{u}_0=-\mathrm{Gr}\,\theta_0\,Cos\alpha-\mathrm{Gm}\,\phi_0 Cos\alpha \tag{12}$$

$$\theta_0''+\Pr\theta_0'-\Pr(F+Q)\theta_0=0 \tag{13}$$

$$\phi_0''+Sc\,\phi_0'-\mathrm{Sc}\,\mathrm{Kr}\,\phi_0=-\mathrm{S_c}\,S_0\,\theta_0'' \tag{14}$$

3.2 First Order Terms

$$\left(1+\frac{1}{\lambda}\right)u_1''+u_1' - (\mathrm{M}^2\, Sin^2\gamma+\mathrm{K}_0)\,\mathrm{u}_1 = -\,\mathrm{Gr}\,\theta_1\, Cos\alpha - \mathrm{Gm}\,\phi_1\, Cos\alpha \tag{15}$$

$$\theta_1''+\Pr\theta_1'+\Pr\left(F+Q\right)\theta_1 = -\Pr(\mathrm{u}_0')^2 - \Pr\mathrm{M}^2\,u_0^2 \tag{16}$$

$$\phi_1''+Sc\,\phi_1' - Sc\,Kr\,\phi_1 = -\mathrm{Sc}\,\mathrm{S}_0\,\theta_1'' \tag{17}$$

The corresponding boundary conditions are

$$\begin{aligned} &u_0 = 0,\ u_1 = 0, \theta_0 = 1, \theta_1 = 0,\ \phi_0 = 1,\quad \phi_1 = 0 \qquad\qquad at \quad y = 0 \\ &u_0 \to 0,\ u_1 \to 0,\ \theta_0 \to 0,\ \theta_1 \to 0, \varphi_0 \to 0,\ \phi_1 \to 0 \qquad as \quad y \to \infty \end{aligned} \tag{18}$$

Solving Eq. (14) – Eq. (19) under the boundary conditions Eq. (20), the following solutions are obtained

$$\theta_0 = \exp(-l_1 y) \tag{19}$$

$$\phi_0 = b_1\exp(-l_1 y)+b_2\exp(-l_2 y) \tag{20}$$

$$u_0 = b_3\exp(-l_1 y)+b_4\exp(-l_2 y)+b_5\exp(-l_3 y) \tag{21}$$

$$\begin{aligned} \theta_1 = {} & b_6\exp(-2l_1 y)+b_7\exp(-2l_2 y)+b_8\exp(-2l_3 y)+b_9\exp(-(l_1+l_2)y)+b_{10}\exp(-(l_3+l_2)y) \\ & +b_{11}\exp(-(l_1+l_3)y)+b_{12}\exp(-l_4 y) \end{aligned} \tag{22}$$

$$\begin{aligned} \phi_1 = {} & b_{13}\exp(-l_4 y)+b_{14}\exp(-2l_1 y)+b_{15}\exp(-2l_2 y)+b_{16}\exp(-2l_3 y)+b_{17}\exp(-(l_1+l_2)y) \\ & +b_{18}\exp(-(l_3+l_2)y)+b_{19}\exp(-(l_1+l_3)y)+b_{20}\exp(-l_5 y) \end{aligned} \tag{23}$$

$$\begin{aligned} u_1 = {} & b_{21}\exp(-l_4 y)+b_{22}\exp(-2l_1 y)+b_{23}\exp(-2l_2 y)+b_{24}\exp(-2l_3 y)+b_{25}\exp(-(l_1+l_2)y) \\ & +b_{26}\exp(-(l_3+l_2)y)+b_{27}\exp(-(l_1+l_3)y)+b_{28}\exp(-l_5 y)+b_{29}\exp(-l_6 y) \end{aligned} \tag{24}$$

Substituting Eq. (19) – Eq. (24) in Eq. (11), we obtain the velocity, temperature and concentration distribution in the boundary layer as follows

$$\begin{aligned} u(y,t) = {} & b_3\exp(-l_1 y)+b_4\exp(-l_2 y)+b_5\exp(-l_3 y)+E_c[b_{21}\exp(-l_4 y)+b_{22}\exp(-2l_1 y)+ \\ & b_{23}\exp(-2l_2 y)+b_{24}\exp(-2l_3 y)+b_{25}\exp(-(l_1+l_2)y)+b_{26}\exp(-(l_3+l_2)y)+ \\ & b_{27}\exp(-(l_1+l_3)y)+b_{28}\exp(-l_5 y)+b_{29}\exp(-l_6 y)] \end{aligned} \tag{25}$$

$$\begin{aligned} \theta(y,t) = {} & \exp(-l_1 y)+E_c[b_6\exp(-2l_1 y)+b_7\exp(-2l_2 y)+b_8\exp(-2l_3 y)+b_9\exp(-(l_1+l_2)y)+ \\ & b_{10}\exp(-(l_3+l_2)y)+b_{11}\exp(-(l_1+l_3)y)+b_{12}\exp(-l_4 y)] \end{aligned} \tag{26}$$

$$\phi(y,t) = b_1 \exp(-l_1 y) + b_2 \exp(-l_2 y) + E_c[b_{13} \exp(-l_4 y) + b_{14} \exp(-2l_1 y) + b_{15} \exp(-2l_2 y) + b_{16} \exp(-2l_3 y) + b_{17} \exp(-(l_1 + l_2) y) + b_{18} \exp(-(l_3 + l_2) y) + b_{19} \exp(-(l_1 + l_3) y) + b_{20} \exp(-l_5 y)] \quad (27)$$

3.3 Skin Friction

The non-dimensional skin friction at the surface is given by

$$\tau = \left(\frac{\partial u}{\partial y}\right)_{y=0}$$

$$= \left(\frac{\partial u_0}{\partial y}\right)_{y=0} + E_c \left(\frac{\partial u_1}{\partial y}\right)_{y=0}$$

$$\tau = -(b_3 l_1 + b_4 l_2 + b_5 l_3) - E_c[b_{21}\, l_4 + 2b_{22} l_1 y + 2b_{23}\, l_2 + 2b_{24}\, l_3 + b_{25}(l_1 + l_2) + b_{26}(l_3 + l_2) + b_{27}(l_1 + l_3) + b_{28}\, l_5 + b_{29} l_6 y)] \quad (28)$$

3.4 Nusselt Number

The rate of heat transfer in terms of the Nusselt number is given by

$$N_u = \left(\frac{\partial \theta}{\partial y}\right)_{y=0}$$

$$= \left(\frac{\partial \theta_0}{\partial y}\right)_{y=0} + E_c \left(\frac{\partial \theta_1}{\partial y}\right)_{y=0}$$

$$= -l_1 - E_c[2b_6\, l_1 + 2b_7\, l_2 + 2b_8\, l_3 + b_9(l_1 + l_2) + b_{10}(l_3 + l_2) + b_{11}(l_1 + l_3) + b_{12}\, l_4] \quad (29)$$

3.5 Sherwood Number

The rate of mass transfer on the wall in terms of Sherwood number is given by

$$Sh = \left(\frac{\partial \phi}{\partial y}\right)_{y=0}$$

$$= \left(\frac{\partial \phi_0}{\partial y}\right)_{y=0} + \left(\frac{\partial \phi_1}{\partial y}\right)_{y=0}$$

$$= -(b_1 l_1 + b_2 l_2) - E_c[b_{13}\, l_4 + 2b_{14}\, l_1 + 2b_{15}\, l_2 + 2b_{16}\, l_3 + b_{17}(l_1 + l_2) + b_{18}(l_3 + l_2) + b_{19}(l_1 + l_3) + b_{20}\, l_5] \quad (30)$$

4. Results and Discussion

The results are showing the nature of the effects of the parameters like inclined parameter α, magnetic field parameter, M, permeability of porous medium, Ko, thermal Grashof number, Gr, mass Grashof number, Gm, Prandtl number, λ is the casson fluid parameter, F is the thermal radiation, Pr, Eckert number, Ec, heat generation parameter, Q, Schmidt number, Sc, chemical reaction, Kr and Soret number So. In the present study, the following default parameter values are adopted for computations: Gr = 5.0, F=0.5, α=30, Gm 5.0, Ko= 1.0, M = 1.0, Pr= 0.71, Ec = 0.01, Q =0.1, Sc= 0.6, Kr = 0.1, So= 0.5. All graphs therefore correspond to these values unless specifically indicated in the appropriate $\frac{\pi}{6}, \frac{\pi}{4}, \frac{\pi}{3}$

4.1 Velocity Profiles

Figure 2 shows the effects of Aligned magnetic field parameter α on velocity profile. We observed that the velocity increases for increasing values of the aligned magnetic field parameter α. The effect of thermal Grashof number Gr on velocity is shown in Figure 3. This figure shows that the fluid velocity increases with increasing values of Gr. This is due to the presence of buoyancy effect which enhances the velocity. In Figure 4 the effects of magnetic parameter M on velocity is shown. From this figure we observed that the velocity decreases as the values of M increasing in case of cooling of the plate. This due to fact of that the transversely applied magnetic field, which has the tendency of slow down the velocity, this force is known as Lorentz force. In Figure 5 the velocity profiles are shown against the span wise coordinate in the presence of permeability parameter. We notice that velocity decreases as permeability parameter Ko. In Figure 6 the velocity profiles are shown against the modified Grashof number. We notice that velocity increases as modified Grashof number Gm increases. Figure 7 elucidates the effect of the velocity profiles for different values of the chemical reaction parameter (Kr). In Figure 8 we observe that velocity decreases as Schmidt number Sc increases. The effects of Soret parameter So on velocity distribution are presented in Figure 9, from this figure we noticed that the velocity increases as Soret Parameter increases.

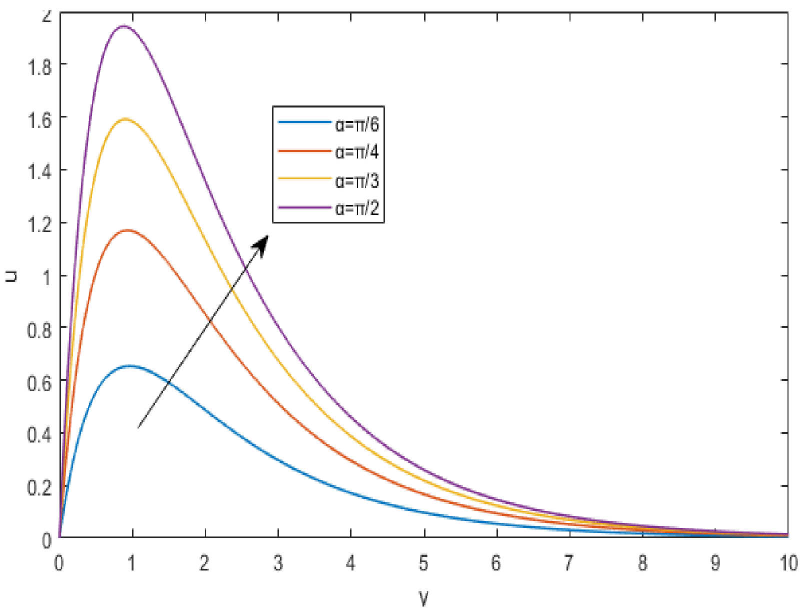

Fig. 2. Velocity profiles for different values of α. So=0.5, Sc=0.6, Pr=0.71, Gr=5, Ko=1, Kr=0.1,M=1, Q=0.1, R=1, Gm=5, Ec=0.001

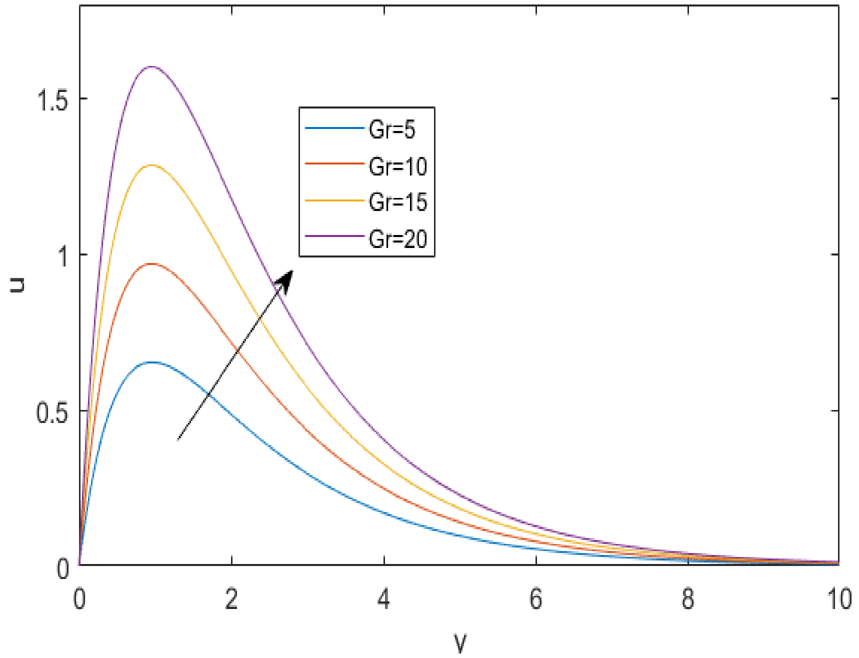

Fig. 3. Velocity profiles for different values of Gr. So=0.5, Sc=0.6, Pr=0.71, Ko=1, α=30, Kr=0.1, M=1, Q=0.1, R=1, Gm=5, Ec=0.00

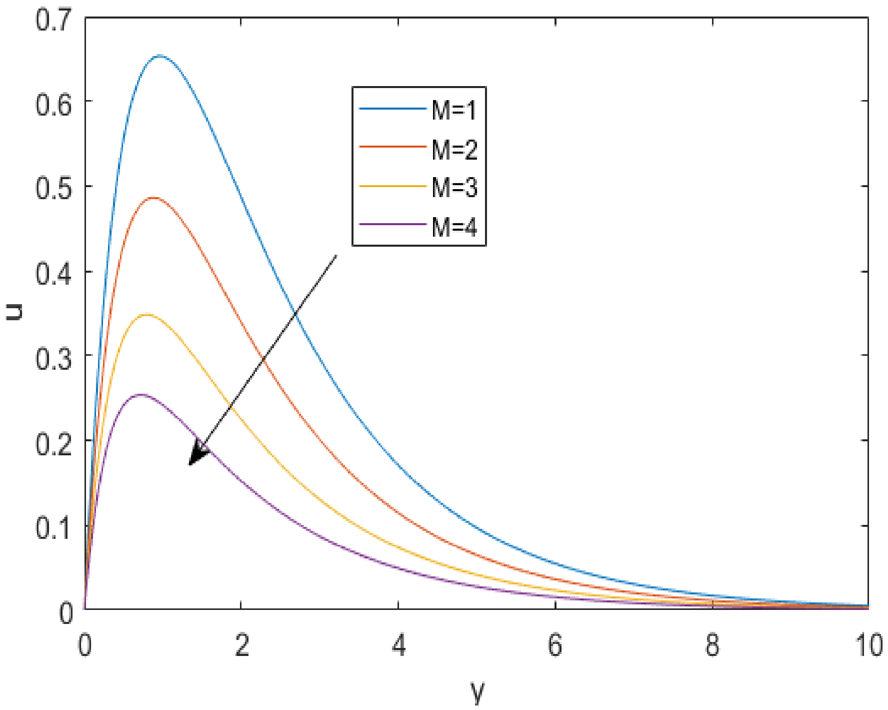

Fig. 4. Velocity profiles for different values of M. So=0.5, Sc=0.6, Pr=0.71, Ko=1, α=30, Kr=0.1, Gr=5, Q=0.1, R=1, Gm=5, Ec=0.001

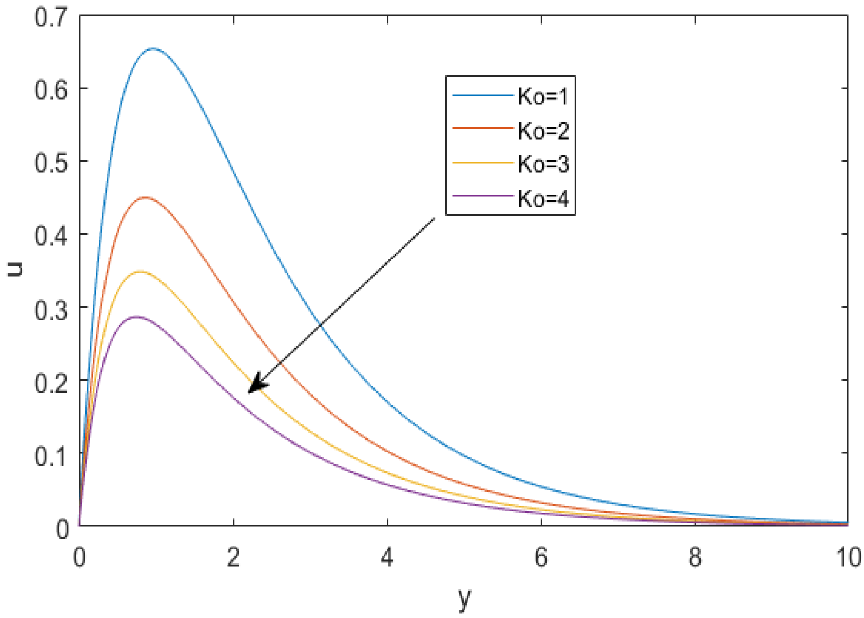

Fig. 5. Velocity profiles for different values of Ko. So=0.5, M=1, Sc=0.6, Pr=0.71, α=30, Kr=0.1, Gr=5, Q=0.1, R=1, Gm=5, Ec=0.001

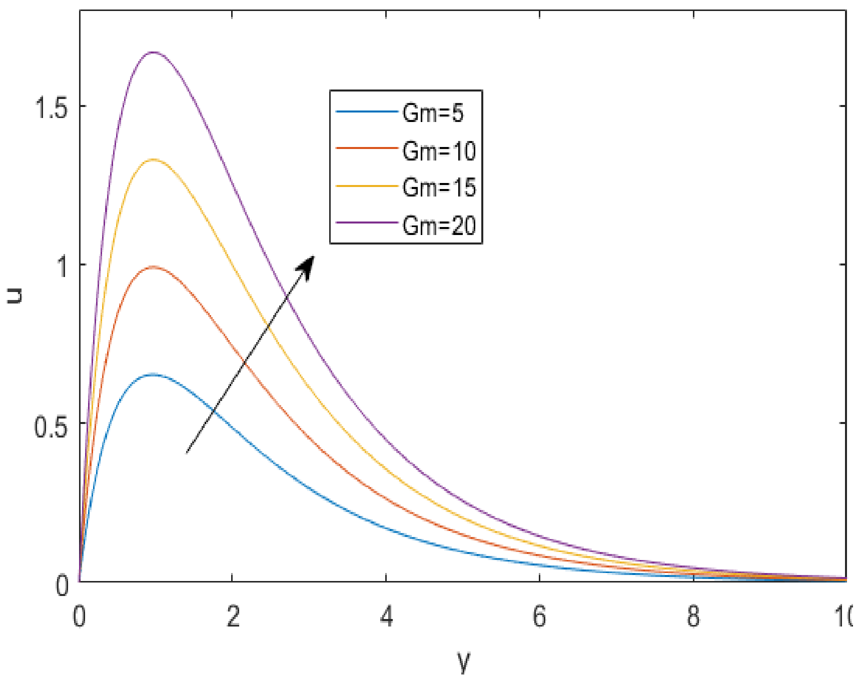

Fig. 6. Velocity profiles for different values of Gm. So=0.5, M=1, Sc=0.6, Pr=0.71, Ko=1, α=30, Kr=0.1, Gr=5, Q=0.1, R=1, Ec=0.001

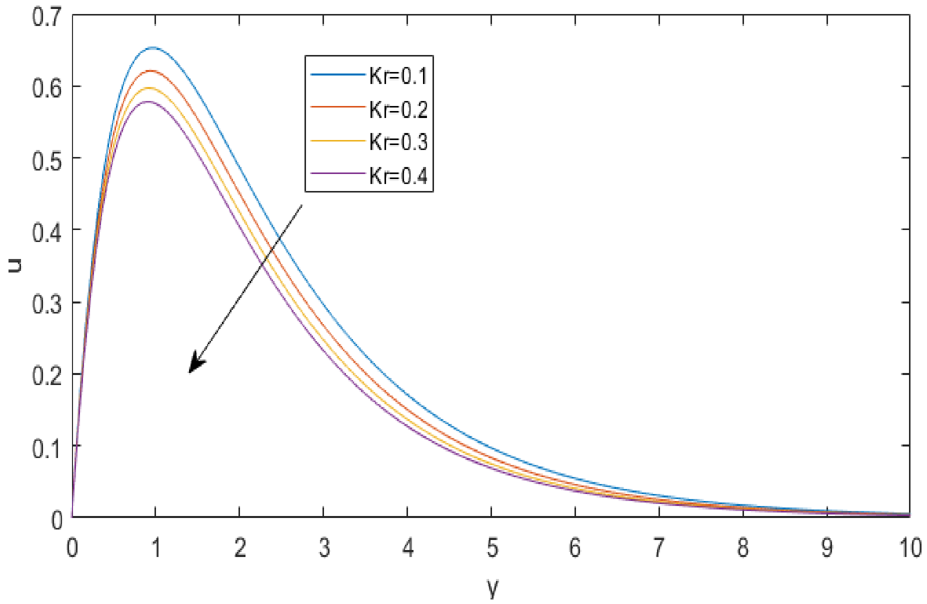

Fig. 7. Velocity profiles for different values of Kr. So=0.5, M=1, Sc=0.6, Pr=0.71, Ko=1, α=30, Gr=5, Q=0.1, R=1, Gm=5, Ec=0.001

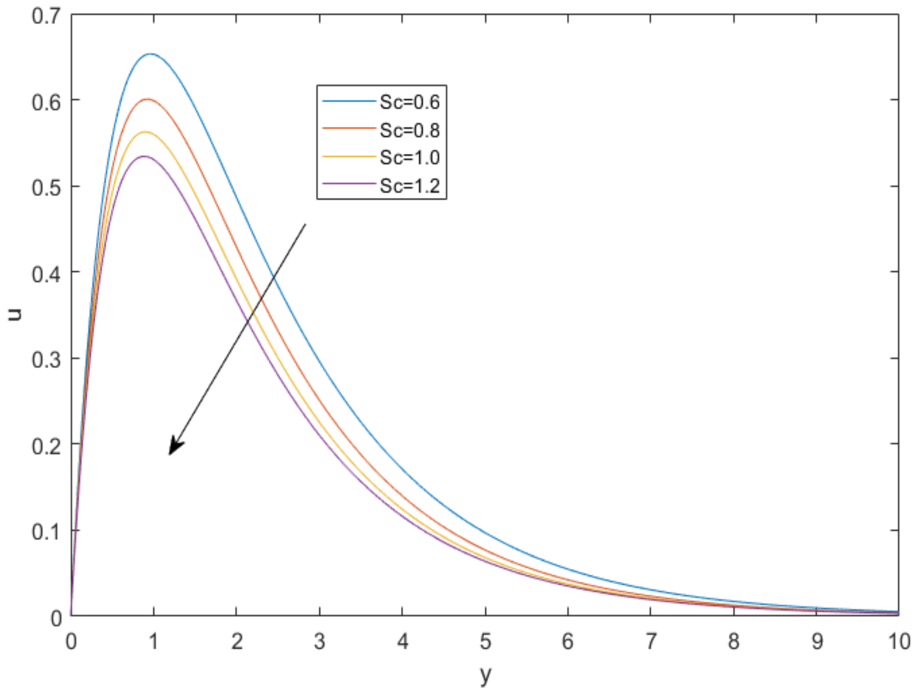

Fig. 8. Velocity profiles for different values of **Sc.** So=0.5, M=1, Pr=0.71, Ko=1, α=30, Kr=0.1, Gr=5, Q=0.1, R=1, Gm=5, Ec=0.001

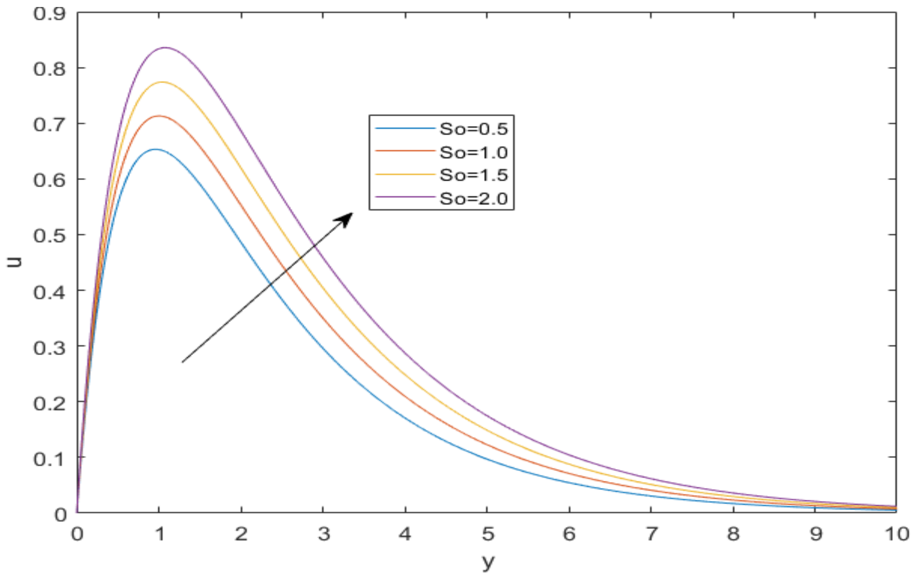

Fig. 9. Velocity profiles for different values of So. M=1, Sc=0.6, Pr=0.71, Ko=1, α=30, Kr=0.1, Gr=5, Q=0.1, R=1, Gm=5, Ec=0.001

4.2 Temperature Profiles

The effects of and heat source/sink parameter Q and prandtl number Pr of on the temperature is presented in the Figure 10 and Figure 11 respectively. Effect of heat source parameter Q on temperature distribution is presented in Figure 10. It is observed that the temperature decreases as an increasing the heat source parameter Q. Figure 11 illustrates the temperature profiles for different values of Prandtl number. It is observed that the temperature decrease as an increasing the Prandtl number. The reason is that smaller values of Prandtl number are equivalent to increase in the thermal conductivity of the fluid and therefore heat is able to diffuse away from the heated surface more rapidly for higher values of Prandtl number.

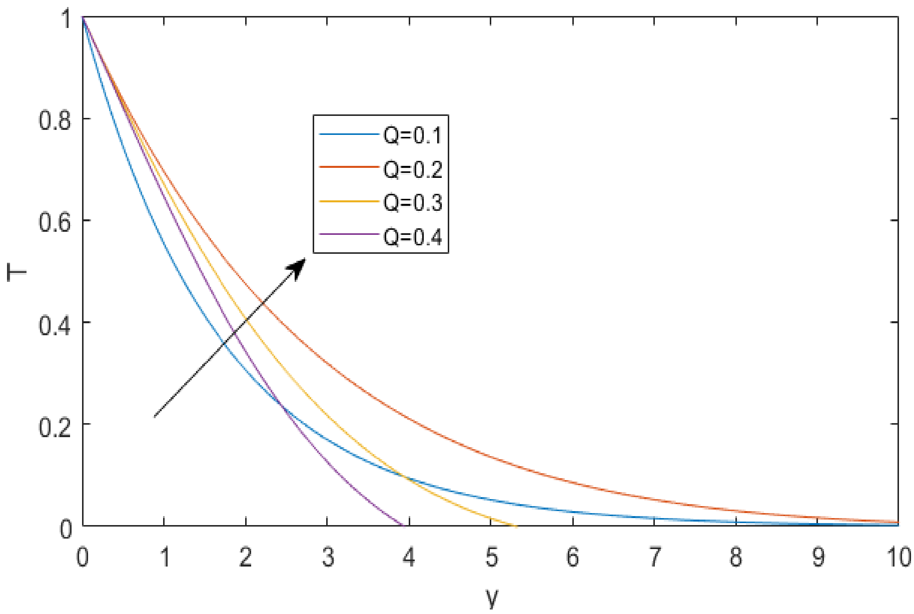

Fig. 10. Temperature profiles for different values of Q. So=0.5, M=1, Sc=0.6, Pr=0.71, Ko=1, α=30, Kr=0.1, Gr=5, R=1, Gm=5, Ec=0.001

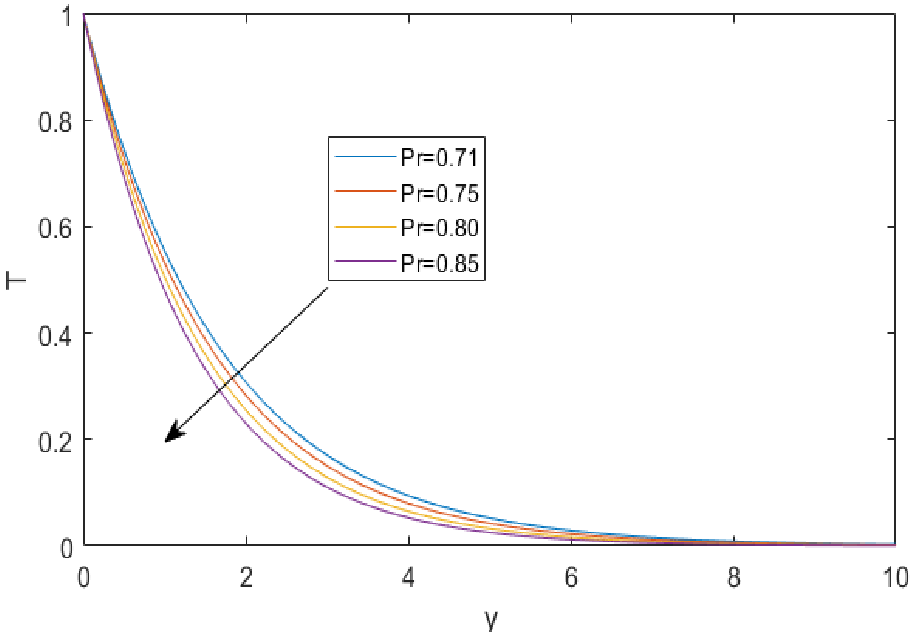

Fig. 11. Temperature profiles for different values of Pr. So=0.5, M=1, Sc=0.6, Q=0.1, Ko=1, α=30, Kr=0.1, Gr=5, R=1, Gm=5, Ec=0.001

4.3 Concentration Profiles

In Figures 12, 13 and 14 the influence of Chemical reaction parameter Kr, Schmidt number sc, and Soret number So, on the species concentration is presented.

Figure12 illustrate the concentration profiles for different values of chemical reaction Kr. From this figure, it is observed that the concentration increases with increasing values of chemical reaction parameter Kr. Figure 13 shows that species concentration profiles for different values of Schmidt number Sc. It is clear that the concentration boundary layer thickness decreases with Sc, also noticed that concentration decreases exponentially and attains free stream condition for large values of Sc. Finally Figure 14 we observed that the concentration is increases with increasing values of soret parameter.

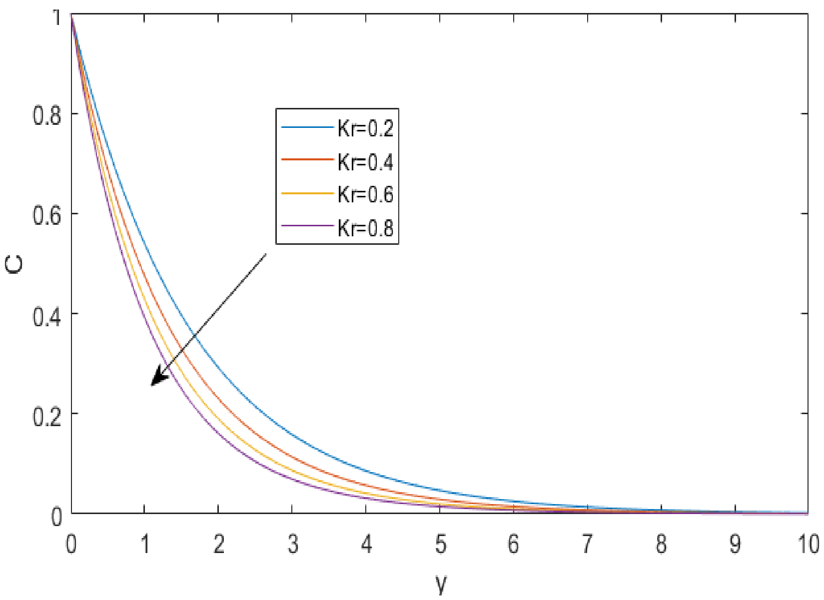

Fig. 12. Concentration profiles for different values of Kr

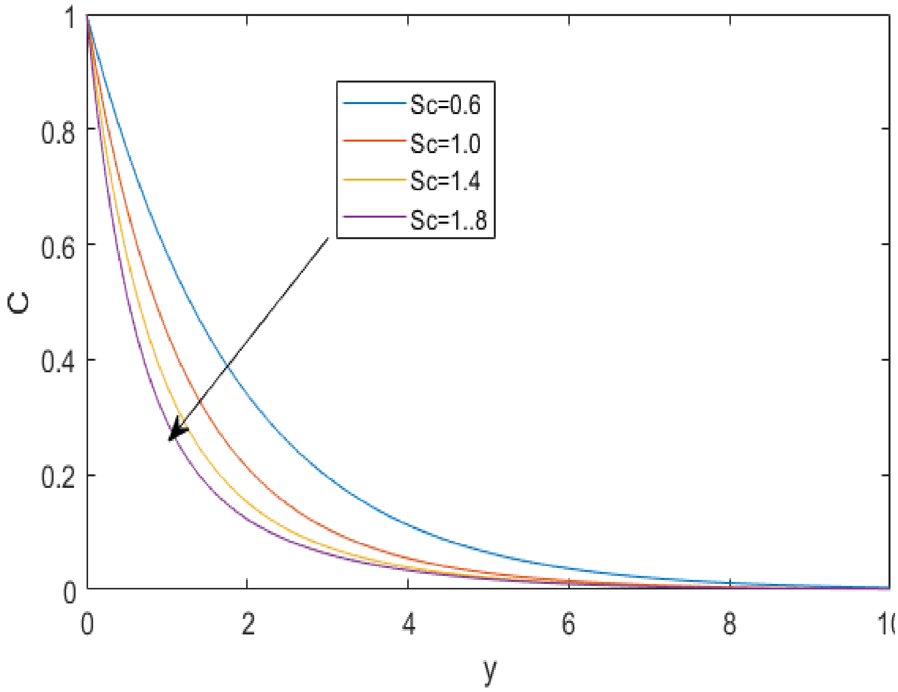

Fig. 13. Concentration profiles for different values of Sc

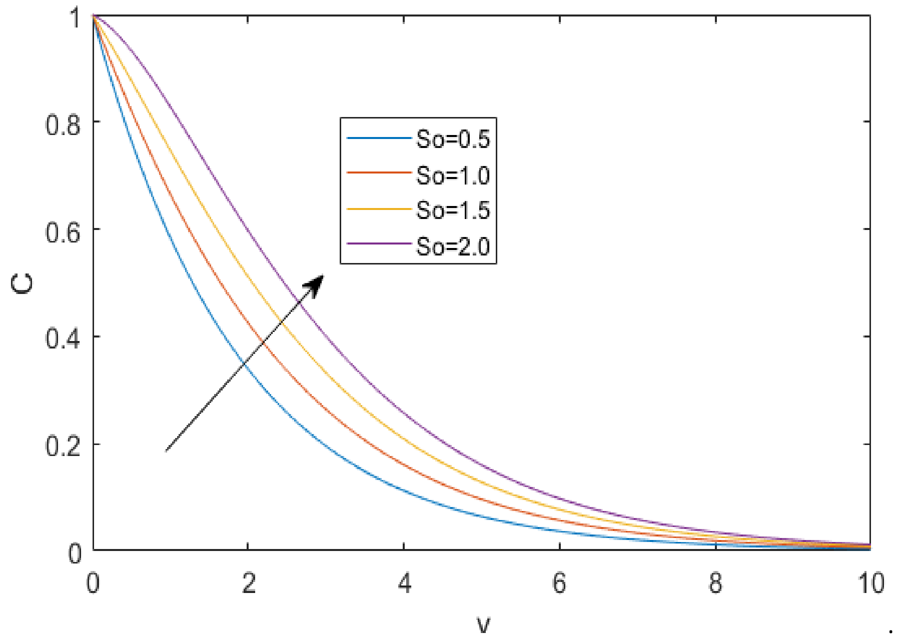

Fig. 14. Concentration profiles for different values of So

Table 1, shows numerical values of skin-friction for several of Grashof number (Gr), modified Grashof number (Gc), Magnetic parameter (M), Porosity parameter (Ko) and Inclined angle (α). From table 1, we observe that the skin-friction increases with an increase in Grashof number (Gr), modified Grashof number (Gc) and Porosity parameter (K) where as it decreases under the influence of magnetic parameter and inclined angle.

Table 1
Skin friction (τ)

Gr	Gm	M	Ko	A	T
5					6.2828
10					9.0189
15					11.7599
	6				6.9902
	12				11.1620
	15				13.1772
		1.5			4.9730
		2			4.0174
		2.5			3.3332
			1.5		5.6489
			2.5		4.7953
			3.5		4.2342
				π/10	6.8989
				π/6	6.2826
				π/3	3.6283

Table 2 demonstrates the numerical values of Nusselt number (Nu) for different values of Prandtl number (Pr), Eckert Number (Ec), Heat absorption parameter (Q) and Magnetic field parameter (M). From Table 2, we notice that the Nusselt number increases with an increase in Prandtl number and Eckert Number where as it decreases under the influence of Heat absorption parameter and Magnetic field parameter.

Table 2
Nusselt number (Nu)

Pr	Ec	M	Q	Nu
0.78				0.00150
0.79				4..5391
0.80				4.1840
	0.01			0.5888
	0.05			5.3022
	0.1			11.1940
		1.5		-0.5397
		2		-0.5668
		2.5		-0.5781
			0.1	-0.4717
			0.15	-0.5144
			0.20	-0.5366

Table 3 shows numerical values of Sherwood number (Sh) for the distinction values of Schmidt number (Sc) and Chemical reaction parameter (Kr) and Soret parameter (So). It can be noticed from Table 3 that the Sherwood number enhances with rising values of Soret Parameter and where as decrease with enhancing the values of Schmidt number and the Chemical reaction parameter.

Table 3
Sherwood number (Sh)

Sc	So	Kr	Sh
0.6			-0.6145
1.2			-1.1013
1.8			-2.5014
	0.5		-0.6145
	1.0		-0.4529
	1.5		-0.2608
		0.001	0.3581
		0.003	0.1430
		0.005	0.0052

5. Conclusion

The effect of Heat Source/Sink effects on Convective flow of a Newtonian fluid past an inclined vertical plate in conducting field is analyzed. The governing equations for the velocity field, temperature and concentration by perturbation technique in terms of dimensionless parameters. The findings of this study are as follows.

i. Velocity decreases for increasing values of the angle of inclination α, magnetic parameter M, chemical reaction parameter Kr and Schmidt number Sc where as it shows reverse tendency in the case of Grashof number Gr, permeability parameter Ko, modified Grashof number Gm and Soret parameter So.
ii. Temperature distribution decreases with an increase in heat Source parameter Q and Prandtl number Pr.
iii. Concentration boundary layer decreases with an increase in Porus medium Ko and Schmidt number Sc where as it is increases with increasing values of Soret Parameter So.
iv. Skin friction increases with an increase of Gr, Gm and Ko but a reverse effect is noticed in the case of M and α.
v. Nusselt number increases as Pr and Ec increases but in the case of M and Q it is decreases.
vi. Sherwood number increases with an increase in So but a reverse effect is noticed in the case of Sc and Kr.

References

[1] Kodi, Raghunath, Mohana Ramana Ravuri, V. Veeranna, M. Ijaz Khan, Sherzod Abdullaev, and Nissren Tamam. "Hall current and thermal radiation effects of 3D rotating hybrid nanofluid reactive flow via stretched plate with internal heat absorption." *Results in Physics* 53 (2023): 106915.. https://doi.org/10.1016/j.rinp.2023.106915

[2] Kodi, Raghunath, Ramachandra Reddy Vaddemani, M. Ijaz Khan, Sherzod Shukhratovich Abdullaev, Attia Boudjemline, Mohamed Boujelbene, and Yassine Bouazzi. "Unsteady magneto-hydro-dynamics flow of Jeffrey fluid through porous media with thermal radiation, Hall current and Soret effects." *Journal of Magnetism and Magnetic Materials* 582 (2023): 171033. https://doi.org/10.1016/j.jmmm.2023.171033

[3] Raju, Konduru Venkateswara, Ravuri Mohanaramana, S. Sudhakar Reddy, and Kodi Raghunath. "Chemical Radiation and Soret Effects on Unsteady MHD Convective Flow of Jeffrey Nanofluid Past an Inclined Semi-Infinite Vertical Permeable Moving Plate." *Communications in Mathematics and Applications* 14, no. 1 (2023): 237. https://doi.org/10.26713/cma.v14i1.1867

[4] Vaddemani, Ramachandra Reddy, Sreedhar Ganta, and Raghunath Kodi. "Effects of Hall Current, Activation Energy and Diffusion Thermo of MHD Darcy-Forchheimer Casson Nanofluid Flow in the Presence of Brownian Motion and Thermophoresis." *Journal of Advanced Research in Fluid Mechanics and Thermal Sciences* 105, no. 2 (2023): 129-145. https://doi.org/10.37934/arfmts.105.2.129145

[5] Raghunath, Kodi, Ravuri Mohana Ramana, Charankumar Ganteda, Prem Kumar Chaurasiya, Damodar Tiwari, Rajan Kumar, Dharam Buddhi, and Kuldeep Kumar Saxena. "Processing to pass unsteady MHD flow of a second-grade fluid through a porous medium in the presence of radiation absorption exhibits Diffusion thermo, hall and ion slip effects." *Advances in Materials and Processing Technologies* (2023): 1-18. https://doi.org/10.1080/2374068X.2023.2191450

[6] Li, Shuguang, Kodi Raghunath, Ayman Alfaleh, Farhan Ali, A. Zaib, M. Ijaz Khan, Sayed M. ElDin, and V. Puneeth. "Effects of activation energy and chemical reaction on unsteady MHD dissipative Darcy–Forchheimer squeezed flow of Casson fluid over horizontal channel." *Scientific Reports* 13, no. 1 (2023): 2666. https://doi.org/10.1038/s41598-023-29702-w

[7] Suresh Kumar, Y., Shaik Hussain, K. Raghunath, Farhan Ali, Kamel Guedri, Sayed M. Eldin, and M. Ijaz Khan. "Numerical analysis of magnetohydrodynamics Casson nanofluid flow with activation energy, Hall current and thermal radiation." *Scientific Reports* 13, no. 1 (2023): 4021. https://doi.org/10.1038/s41598-023-28379-5

[8] Raghunath, K., R. Mohana Ramana, V. Ramachandra Reddy, and M. Obulesu. "Diffusion Thermo and Chemical Reaction Effects on Magnetohydrodynamic Jeffrey Nanofluid Over an Inclined Vertical Plate in the Presence of Radiation Absorption and Constant Heat Source." *Journal of Nanofluids* 12, no. 1 (2023): 147-156. https://doi.org/10.1166/jon.2023.1923

[9] Maatoug, Samah, K. Hari Babu, V. V. L. Deepthi, Kaouther Ghachem, Kodi Raghunath, Charankumar Ganteda, and Sami Ullah Khan. "Variable chemical species and thermo-diffusion Darcy–Forchheimer squeezed flow of Jeffrey nanofluid in horizontal channel with viscous dissipation effects." *Journal of the Indian Chemical Society* 100, no. 1 (2023): 100831. https://doi.org/10.1016/j.jics.2022.100831

[10] Bafakeeh, Omar T., Kodi Raghunath, Farhan Ali, Muhammad Khalid, El Sayed Mohamed Tag-ElDin, Mowffaq Oreijah, Kamel Guedri, Nidhal Ben Khedher, and Muhammad Ijaz Khan. "Hall current and Soret effects on unsteady MHD rotating flow of second-grade fluid through porous media under the influences of thermal radiation and chemical reactions." *Catalysts* 12, no. 10 (2022): 1233. https://doi.org/10.3390/catal12101233

[11] Deepthi, V. V. L., Maha MA Lashin, N. Ravi Kumar, Kodi Raghunath, Farhan Ali, Mowffaq Oreijah, Kamel Guedri, El Sayed Mohamed Tag-ElDin, M. Ijaz Khan, and Ahmed M. Galal. "Recent development of heat and mass transport in the presence of Hall, ion slip and thermo diffusion in radiative second grade material: application of micromachines." *Micromachines* 13, no. 10 (2022): 1566. https://doi.org/10.3390/mi13101566

[12] Ganjikunta, Aruna, Hari Babu Kommaddi, Venkateswarlu Bhajanthri, and Raghunath Kodi. "An unsteady MHD flow of a second-grade fluid passing through a porous medium in the presence of radiation absorption exhibits Hall and ion slip effects." *Heat Transfer* 52, no. 1 (2023): 780-806. https://doi.org/10.1002/htj.22716

[13] Raghunath, Kodi, and Ravuri Mohanaramana. "Hall, Soret, and rotational effects on unsteady MHD rotating flow of a second-grade fluid through a porous medium in the presence of chemical reaction and aligned magnetic field." *International Communications in Heat and Mass Transfer* 137 (2022): 106287. https://doi.org/10.1016/j.icheatmasstransfer.2022.106287

[14] Kodi, Raghunath, Mohanaramana Ravuri, Nagesh Gulle, Charankumar Ganteda, Sami Ullah Khan, and M. Ijaz Khan. "Hall and ion slip radiative flow of chemically reactive second grade through porous saturated space via perturbation approach." *Waves in Random and Complex Media* (2022): 1-17. https://doi.org/10.1080/17455030.2022.2108555

[15] Vaddemani, Ramachandra Reddy, Raghunath Kodi, and Obulesu Mopuri. "Characteristics of MHD Casson fluid past an inclined vertical porous plate." *Materials Today: Proceedings* 49 (2022): 2136-2142. https://doi.org/10.1016/j.matpr.2021.08.328

[16] Kodi, Raghunath, Ramachandra Reddy Vaddemani, and Obulesu Mopuri. "Effects of radiation absorption and aligned magnetic field on MHD Cassion fluid past an inclined vertical porous plate in porous media." *Simulation and Analysis of Mathematical Methods in Real-Time Engineering Applications* (2021): 273-291. https://doi.org/10.1002/9781119785521.ch12

[17] Reddy, T. S., M. C. Raju, and S. V. K. Varma. "Unsteady MHD radiative and chemically reactive free convection flow near a moving vertical plate in porous medium." (2013): 443-451.

[18] Raju, K. V. S., T. Sudhakar Reddy, M. C. Raju, PV Satya Narayana, and S. Venkataramana. "MHD convective flow through porous medium in a horizontal channel with insulated and impermeable bottom wall in the presence of viscous dissipation and Joule heating." *Ain Shams Engineering Journal* 5, no. 2 (2014): 543-551. https://doi.org/10.1016/j.asej.2013.10.007

[19] Ravikumar, V., M. C. Raju, and G. S. S. Raju. "Combined effects of heat absorption and MHD on convective Rivlin-Ericksen flow past a semi-infinite vertical porous plate with variable temperature and suction." *Ain Shams Engineering Journal* 5, no. 3 (2014): 867-875. https://doi.org/10.1016/j.asej.2013.12.014

[20] Raju, M. C., N. Ananda Reddy, and S. V. K. Varma. "Analytical study of MHD free convective, dissipative boundary layer flow past a porous vertical surface in the presence of thermal radiation, chemical reaction and constant suction." *Ain Shams Engineering Journal* 5, no. 4 (2014): 1361-1369. https://doi.org/10.1016/j.asej.2014.07.005